



The influence of fish bone morphology on aquatic transport: An experimental approach through elements of Creole perch (Percichthyidae: *Percichthys trucha*; [Valenciennes, 1833])



M. Corbat^{a,*}, M. Giardina^b, A.F. Zangrando^{c,d}

^a IESyPPat-CONICET, Universidad Nacional de la Patagonia San Juan Bosco, Ciudad Universitaria Km 4, 9000 Comodoro Rivadavia, Chubut, Argentina

^b IANIGLA-CONICET, Museo de Historia Natural de San Rafael, Av. Ballofet s/n, Parque Mariano Moreno, 5600 San Rafael, Mendoza, Argentina

^c CADIC-CONICET, Bernardo Houssay 200, V9410CAB Ushuaia, Tierra del Fuego, Argentina

^d Universidad de Buenos Aires, Facultad de Filosofía y Letras, Argentina

ARTICLE INFO

Keywords:

Bone morphology
Hydrodynamic transport
Sphericity index
Taphonomy
Zooarchaeology
Fish remains
Experimentation

ABSTRACT

Many archaeological sites with fish remains are situated near ancient or current water courses. The origin of these time-averaged contexts requires an analysis considering possible non-human contributions and specifically the role of water as a highly selective agent. Element shape is a critical factor in all transport processes, but it has received little attention. The aim of this experimental work is to explore the hydrodynamic transport of fish bones considering the shape of anatomical elements. Different elements from Creole perch (Percichthyidae: *Percichthys trucha*; [Valenciennes, 1833]) individuals are utilized in dry conditions and under three different flow speeds. Transport groups, mode of transport and distance travelled are evaluated according to the shape of the elements. Fish vertebrae have the greatest transport potential. This experimental study indicates that hydrologic processes can impose biases giving a unique skeletal element composition in fish bone assemblages. A simplified differential transport model is proposed and an archaeological application of it is essayed.

1. Introduction

Several researches have evaluated the consequences of water action on bone assemblages through laboratory experiments and observations in natural environments, considering different variables and taxa (Aslan and Behrensmeyer, 1996; Behrensmeyer, 1975; Boaz and Behrensmeyer, 1976; Coard and Dennell, 1995; Coard, 1999; Dodson, 1973; Hanson, 1980; Kaufmann and Gutiérrez, 2004; Kaufmann et al., 2011; Pante and Blumenschine, 2010; Trapani, 1998; Voorhies, 1969). Although hydraulic processes were recognized as potential causes of biased fish assemblages many years ago (Butler, 1996; Nicholson, 1992b; Stewart, 1991), few studies have focused on this topic.

Previous investigations have noted that bone shape strongly influences fluvial as much as terrestrial displacements (Behrensmeyer, 1975; Dodson, 1973; Frostick and Reid, 1983; Kaufmann and Gutiérrez, 2004; Stewart, 1991; Trapani, 1998; Voorhies, 1969). In this sense, spherically shaped bones, such as vertebrae, are more prone to dispersal than those which have less rounded shapes, such as limb bones (Aslan and Behrensmeyer, 1996; Dodson, 1973; Frostick and Reid, 1983). Bone elements with low sphericity index would have, according to their shape, less chances of moving in a fluvial or terrestrial medium than

those with the highest sphericity values (Kaufmann and Gutiérrez, 2004). However, it is important to note that in sedimentological studies a spherical particle can behave differently according to the type of transport implied: in suspension, the particle will tend to deposit, whereas it will move forward under traction conditions. This rests on the fact that a particle's shape can delay or accelerate the falling speed or have an influence on the effectiveness of movements. Thus, transport by traction process is more effective in equant and prolate clasts, whereas suspension has a greater efficacy on oblate and laminar ones.

Although considerable differences in the shape of the same element even within the same fish family have been observed (Colley, 1990), it has also been shown that morphology values are generally similar for the same elements from different taxa (Falabella et al., 1994). Even though some families have specialized and modified parts - particularly near the mouth, the shape of each element can be standardized for most of the taxa (Nagaoka, 2005).

The aim of this experimental work is to explore the hydrodynamic transport of fish bones considering the shape of anatomical elements of Creole perch (Percichthyidae: *Percichthys trucha*; [Valenciennes, 1833]). This species is widely distributed in the Neotropics, and it is part of the Perciformes order, the largest order of fishes in the planetary ecosystem

* Corresponding author.

E-mail addresses: mercedescorbat@yahoo.com.ar (M. Corbat), mgiardina@mendoza-conicet.gov.ar (M. Giardina), afzangrando@cadic-conicet.gov.ar (A.F. Zangrando).

Table 1
Sphericity, shape and quantity of anatomic elements analyzed.

Element		Sphericity		Shape	N
		Mean	SD		
Parasphenoid	Pas	0.20	0.02	Blade	26
Suboperculum	Sop	0.21	0.01	Blade	23
Frontal	Ftl	0.22	0.02	Blade	28
Interoperculum	Iop	0.30	0.02	Blade	24
Pharyngeal	Ph	0.31	0.02	Blade	18
Palatine	Pl	0.31	0.02	Blade	24
Cleithrum	Cl	0.37	0.02	Blade	22
Preoperculum	Pop	0.38	0.02	Disc-blade	23
Posttemporal	Pot	0.39	0.02	Blade	24
Ceratohyal	Crhy	0.39	0.02	Blade	22
Premaxilla	Pmx	0.40	0.02	Blade	18
Maxilla	Mx	0.42	0.02	Rod	22
Articular	Ar	0.43	0.03	Blade	23
Otolith	Ot	0.45	0.05	Blade	25
Dentary	Dn	0.47	0.03	Blade	19
Vomer	V	0.47	0.04	Rod-blade	24
Pharyngeal	ph	0.49	0.02	Blade	20
Orbital	Or	0.50	0.04	Blade-disc	21
Hyomandibular	Hyo	0.50	0.03	Disc	24
Epiphyal	Ephy	0.52	0.04	Disc	23
Operculum	Op	0.54	0.03	Disc	21
Quadrate	Qu	0.59	0.04	Blade-disc	24
Basioccipital	Bso	0.65	0.04	Disc-rod	26
1st vertebra	1st V	0.86	0.09	Sphere	26
Caudal vertebra	CV	1.02	0.06	Sphere	27

Note: distinction between Ph and ph corresponds to lower (fifth ceratobranchial) and upper (third pharyngobranchial) pharyngeal bones, respectively (sensu Wainwright, 2005).

(Wheeler and Jones, 1989: 23). The goal of this article is twofold. Firstly, the shape of fish bones is analyzed and the intra-specific variability in relation to this property is evaluated. Secondly, three sets of experiments - with different hydric flow velocity - are presented in this work, which were conducted with disarticulated dry fishbones in a flume. The implications for taphonomy and archaeology are finally discussed.

2. Materials and methods

The morphology of 25 different anatomic elements belonging to 30 Creole perch individuals was estimated. Elements were obtained from naturally deposited carcasses (Corbat and Zangrando, 2012). Since the majority of the carcasses were incomplete, the amount of samples for each element ranges from 18 to 28, as detailed in Table 1. The average of all measurements taken was calculated for each element and used to estimate shape and sphericity values. The analyzed bone collection is available at the Museo de Historia Natural de San Rafael (Mendoza, Argentina).

In archaeological research at least two methods have been used for estimating elements' morphology. The first one corresponds to "subjective" criteria after a visual evaluation, which can be assigned from value 1, as laminar structures or bones with many ramifications, to value 5, as almost spherical elements (Falabella et al., 1994). It can also be possible to designate bone shape categories according to their general aspect: robust, flat, spherical or irregular (Nicholson, 1992b). The second one is based on sedimentological studies (Blatt et al., 1980; Zingg, 1935) and enables quantitative approaches to an element's shape and sphericity degree - the extent to which its shape resembles a sphere - by considering each one as a sedimentary particle and by means of the relations among its dimensions (Behrensmeier, 1975; Darwent and Lyman, 2002; Frostick and Reid, 1983; Kaufmann and Gutiérrez, 2004; Nagaoka, 2005; Trapani, 1998). This last method is used here for considering more precise and less dependent on individual perceptions.

Three main axes from each analyzed bone were measured with a

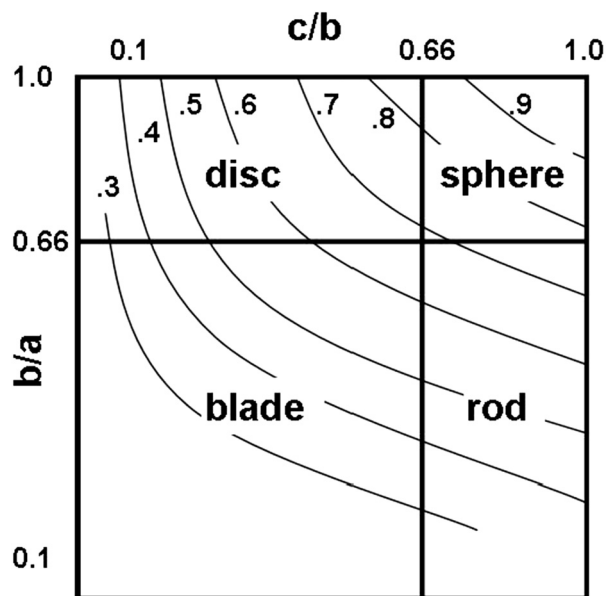


Fig. 1. Classification of elements regarding their shape and sphericity. Curves show sphericity according to the $(bc/a^2)^{0.33}$ formula. Modified from Frostick and Reid (1983).

digital caliper: a. major axis (length), b. intermediate axis (width) and c. minor axis (thickness). These three dimensions - taken on mutually perpendicular axis and considering their maximum values - are used to calculate sphericity with the following equation:

$$(bc/a^2)^{0.33}$$

The ratios b/a and c/b allow classifying elements according to their location in a graph, within four shape classes: spherical or "equidimensional" in the upper right quadrant; disc, tabular or "oblate" in the upper-left; blade, laminar or ellipsoidal in the bottom-left; and rod, cylindrical or "prolate" in the bottom-right one (Zingg, 1935). Sphericity value can also be marked in the graph, so that more spherical elements (with the highest values) will be close to the upper-right corner and less spherical ones will approach the bottom-left angle (Fig. 1).

In order to evaluate the hydric transport of fish bones, 20 anatomical elements corresponding to 4 Creole perch individuals were used in the experiment, making a total of 80 bone elements.

To conduct the experiment, a smooth bottomed channel with a width and length of 0.4 m and 6.0 m respectively, was used. It is made of acrylic and has a rectangular section. This channel was provided by the Universidad Tecnológica Nacional de San Rafael (Mendoza). Hydraulic engineers Roberto Biondi and Nicolás Membrive acquired the hydric flow velocities of 10 cm/s, 33 cm/s and 50 cm/s by a pump and slope regulation.

Low speeds (10 cm/s and 33 cm/s) were chosen as they would be the expectable ones for floodplains adjacent to the main current (Kaufmann et al., 2011) and a higher one (50 cm/s), included in low energy currents ranges, was added in order to explore this variable.¹ If an element did not cross the test section² (50 cm for the lowest speed; 2 m for 33 and 50 cm/s) after three trials, it was considered as not transported at that flow velocity.

Each dry skeletal element free of soft tissue was placed on the centre and bottom of the channel, so that potential turbulence caused by

¹ According to Behrensmeier (1975) flow velocity in natural situations are between 20 and 150 cm/s.

² The lengths of the test sections was arbitrarily determined at 2 m, regarding that a previous experiment on artiodactyla bigger and heavier bones used a test section of 3 m (Kaufmann et al., 2011). As the lowest speed did not show many displacements, test section was shortened at 0.50 cm for that case.

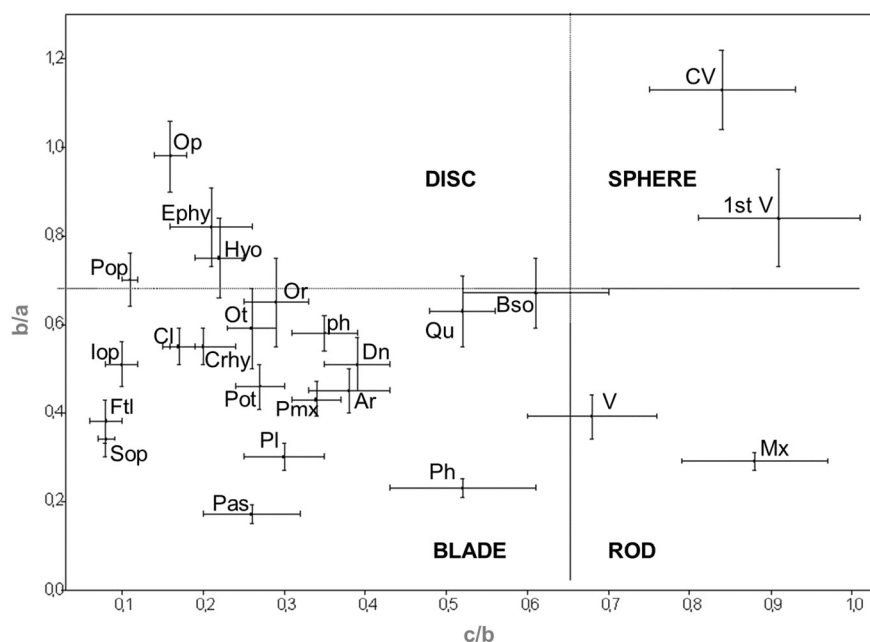


Fig. 2. Classification of Creole perch elements according to ratios c/b and b/a .

surrounding specimens and flow friction on channel walls were minimized. The elements were oriented with long axes parallel to the current and in their more stable position, generally convex-up (Voorhies, 1969).

The time consumed for passing the test section was measured in seconds with a chronometre. These data were transformed to decimal system using Microsoft Office Excel tools. Given that many elements did not move and had not a time measure, we transformed time information as a measure of the distance (cm) covered in a second. Mode of transport of the bone was noted (i.e., rolling, sliding and/or saltation along the bed, and/or floating in the water surface) and most of the trials were also filmed.

Since the data did not meet the requirements for parametric statistical tests, the relation between bone shape and aquatic transport was assessed using Kruskal Wallis test (K-W), followed by the Mann-Whitney U test (Hammer et al., 2001).

3. Results

Table 1 presents the mean values (\pm SD) of sphericity and size sample for each element; measurements for all skeletal units are detailed in Supplemental file 1. The classifications of bone shape according to ratios b/a and c/b are plotted in Fig. 2. Variability in the values of some elements transgresses classes' limits. For that reason, and in order to simplify our analysis, combined shape assignments were considered when $> 25\%$ of the cases could be classified as another shape class.

Even though vertebral centra³ show the biggest variability in their ratios estimations, only these elements were classified as spheres. Maxillas stand out among rod shapes, and so were described for fishes in general (Nagaoka, 2005). This class with intermediate sphericity values also includes vomers, though 35.5% of this element also corresponds to blade shapes. Preoperculum, operculum, epihyals and hyomandibulars are essentially discs. Basioccipitals are mainly classified as discs, but they are rather close to the other shapes boundaries, being also classified as rods or blades in 32% and 24% of the cases, respectively. The 26% of preoperculum falls on bladespectrum.

Most of the elements are blades, with the lowest and intermediate

sphericity values. This class contains most of cranial bones. Parasphenoids, suboperculum, interoperculum and frontals are the least spherical and the most flat bones. Blades also include orbitals, quadrates, otoliths, pharyngeals, cleithrums, ceratohyals, palatines, posttemporals, dentaries, articulars and premaxillas. Orbitals are also represented by discs in almost 48% of the cases. The 24% of the otoliths and 33% of the quadrates are also discs. Quadrate has been classified as a disc-shaped element by Nagaoka (2005), together with the dentary, articular and premaxilla, which are classified as blades by us. This disagreement may be reflecting inter-taxonomic variability.

When relation between shape classification as a qualitative variable (sphere, disc, rod and blade) and sphericity index is evaluated (Fig. 3), it is observed that blades present the lowest sphericity values in contrast to spheres with the highest ones. Even though spheres may overlap discs' outliers,⁴ most of them typically present the highest sphericity values, averaging 0.96. Rods and discs have intermediate values, being the former relatively higher. It is also noted that blades with sphericity values of 0.37 on average cover a rather wide range, which includes sphericity values of rods and discs.

Some variation in hydric behaviour among the same elements from different individuals was detected. We have considered each individual sample as a trial for the element, running four trials for each anatomical unit. Each element from the four skeletons was assigned to one of the following groups, suggesting different hydric displacement possibilities and following a modified Voorhies's (1969) proposal (Table 2). Group 1 (G1): skeletal elements which passed through the testing section in all the four trials. Group 2 (G2): skeletal elements which passed through the testing section in at least one trial, but not all. Group 3 (G3): skeletal elements which did not pass through the testing section in any trial.

The number of transported bone elements increases when velocity raises (Fig. 4). With the fastest speed (50 cm/s), all elements are transported and most of them (80%) moved in all the trials (G1). The main change is observed between the 10 cm/s and 33 cm/s series: with the lowest speed, only 10% of the elements corresponds to G1, 40% to G2 and 50% did not move at all; with the 33 cm/s speed, the opposite tendency is observed (50% belong to G1, 40% to G2 and only 10% to G3).

³ The term "vertebrae" refers to vertebral centra throughout the text.

⁴ The outlier is a vertebra with a sphericity value of 0.86.

Fig. 3. Sphericity index for different shapes.

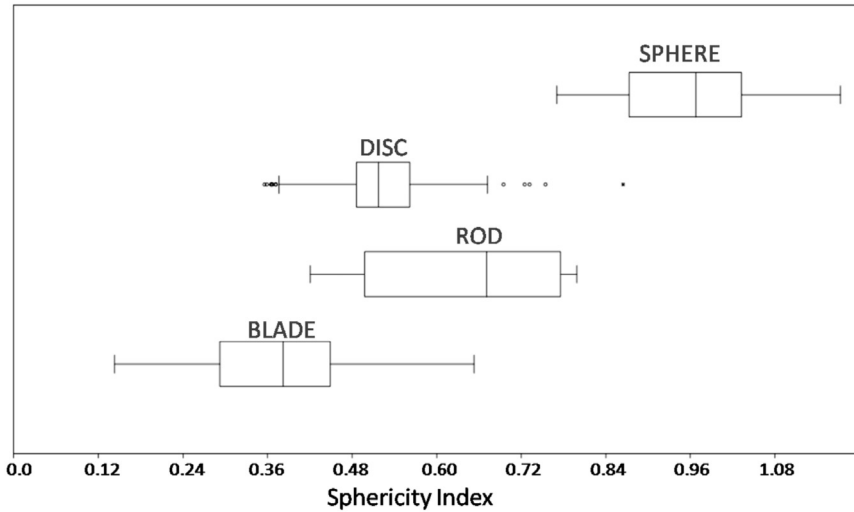


Table 2
Transport group and mode of transport for each element at different flow speeds. Elements are ordered from the highest to the lowest sphericity values. References: G: group of hydric transport potential; MT: modes of transport movements. F: flotation; SL: sliding; S: saltation; R: rolling; x = non-transported.

Element	Flow velocity					
	10 cm/s		33 cm/s		50 cm/s	
	G	MT	G	MT	G	MT
CV	2	F-SL	1	R-S	1	R-S
1st V	1	SL-F	1	SL-S-F	1	S-SL
Bso	2	SL	1	SL-S	1	SL
Qu	2	SL	1	SL	1	SL
Op	3	x	1	SL	1	SL
Ephy	2	SL-F	1	F-SL-S	1	F-SL
Hyo	2	SL	1	SL	1	SL
V	3	x	1	SL	1	SL
Dn	3	x	2	SL	2	SL
Ot	3	x	3	x	2	SL
Ar	1	SL	2	SL	1	SL
Mx	3	x	2	SL	2	SL
Pmx	3	x	2	SL	1	SL
Crhy	2	SL	1	SL-F	1	SL-F
Pot	3	X	2	SL	1	SL
Pop	3	x	2	SL	1	SL
Cl	3	x	2	SL	1	SL
Ph	2	SL-F	1	SL-F	1	SL-F
Ftl	3	x	2	SL	1	SL
Pas	2	SL	3	x	2	SL

4. Discussion

4.1. Assessing experimental results

A visual exploration of Fig. 5 suggests that spheres are the most transportable elements, followed by blades, while rods seem to move less. However, when sphericity values associated with different transport groups are assessed through Kruskal-Wallis and Mann-Whitney's pairwise comparisons, a significant difference is only recorded in the 33 cm/s series ($H = 7.614$; $p < 0.05$), specifically between G1 and G2.

Considering shape classes represented in each transport group, at different current speeds, no pattern is observed (Fig. 6), and contingency tables indicate that there are no significant correlations between shape classes and transport groups (Monte Carlo test: 1. 10 cm/s,

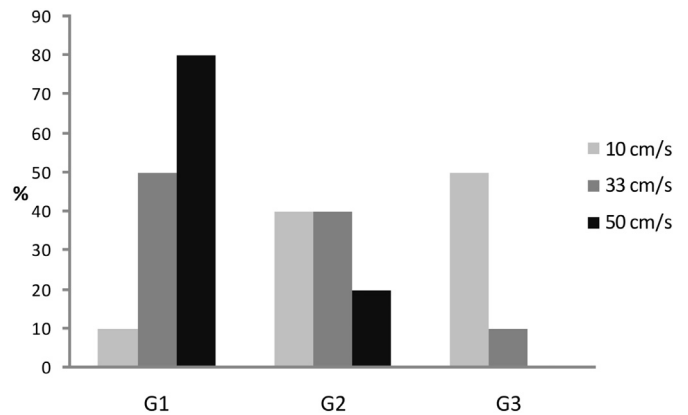


Fig. 4. Relative frequency of elements at different flow speed according to their transport group classification.

$p = 0.39$; 2. 33 cm/s, $p = 0.61$; 3. 50 cm/s, $p = 1$). Shape, either qualitatively or quantitatively described, does not explain transport groups conformation, at least in the terms in which these groups have been defined.

If we consider shape by mode of transport some general trends can be observed. Using the speed series with the highest correlation (50 cm/s), spheres seem to be associated with rolling (R) and saltation (S) movements, while blades do it primarily with sliding (SL), but also with the absence of movement (None). Discs and rods do not present strong associations. Discs are primarily related to sliding, and then to flotation (F); Rods are associated with sliding or no-movements (Fig. 7). Monte Carlo's statistic suggests that there exists a difference between the modes of movements associated with different shape classes (10 cm/s, $p = 0.02$; 33 cm/s, $p = 0.00$; 50 cm/s, $p = 0.00$), which is consistent with previous studies on other fauna classes and sedimentology.

In the same way, using the 50 cm/s series data, boxplot of sphericity values included in each type of movement shows that most spherical elements tend to move by saltation or rolling, while elements with low and medium sphericity values, when transported, do it by flotation or sliding. This trend is also seen in the 33 cm/s series, but not in the lowest one (Fig. 8).

Kruskal-Wallis analysis shows that there exists significant differences ($p < 0.05$) between sphericity values associated with each type of movement in the 33 cm/s ($H = 20.04$) and 50 cm/s series ($H = 17.02$), but not in the lowest one ($H = 2.573$). According to Mann-Whitney's comparison, these significant differences ($p < 0.05$)

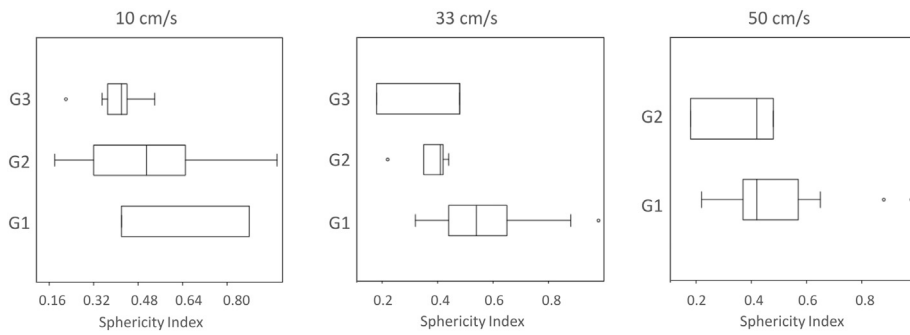


Fig. 5. Sphericity index of each transport group at different flow speeds.

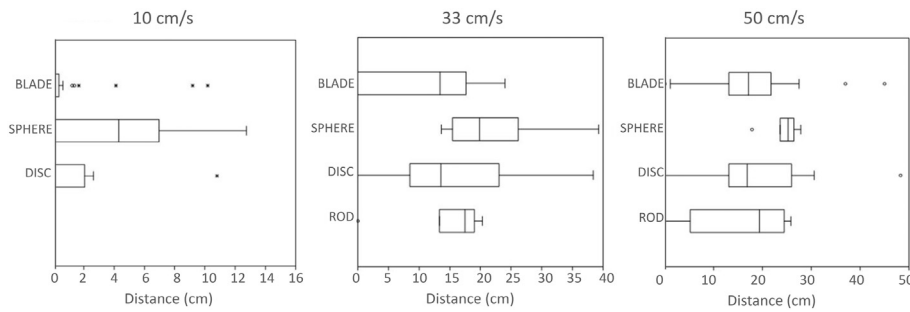


Fig. 6. Shape classes for each transport groups at different flow speeds.

are found between R-SL, R-F, R-None, SL-S. In the 33 cm/s series there were also found significant differences between SL-None and between S-None.

Boxplots relating distances covered by each shape are presented in Fig. 9. Kruskal-Wallis analysis indicates that there exist significant differences ($p < 0.05$) between distances covered by different shape classes in all speed series (10 cm/s: $H = 9.662$; 33 cm/s: $H = 10.29$; 50 cm/s: $H = 9.394$). Mann-Whitney's pairwise comparison indicates that these differences are found between spheres and blades in all the series, between spheres and rods in the 50 cm/s and 10 cm/s series, and between spheres and discs in the latter speed.

Regression tree⁵ applied to sphericity and distances for each flow velocity predicts different groups with significant differences (Fig. 10): For 10 cm/s flow velocity, two groups are predicted and critical sphericity level seems to be 0.65. For 33 cm/s series, three groups are predicted, showing a greater variability. The threshold of 0.58 indicates a significant difference in 33 and 50 cm/s speeds; when sphericity values are bigger than 0.58, all elements are transported and variability decreases. Then, flow velocity increases fish bone transport potential mainly when sphericity is > 0.58 .

4.2. Implications for ichthyarchaeological studies

Relative differences between anatomical parts may provide useful information in interpretations of cultural patterns in the use of fish resources (Butler, 1993, 1996; Gifford-Gonzalez et al., 1999; Stewart, 1991; Stewart and Gifford-Gonzalez, 1994; Stewart et al., 1997; Wheeler and Jones, 1989; Zohar and Cooke, 1997; Zohar et al., 2001). Other potential processes of differential representation in fish body parts were also recognized as possible explanations, like methodological bias in recovery (Butler, 1996; Falabella et al., 1994; Grayson, 1988; Lyman, 1984, 1985; Nagaoka, 2005; Stahl, 1996; Wheeler and Jones, 1989; Zohar and Belmaker, 2005) or differential preservation (Butler and Chatters, 1994; Lubinski, 1996; Nicholson, 1992a, b, 1993, 1996, 1998; Zohar and Biton, 2011; Zohar et al., 2008). However, the effects of hydrologic processes have not been widely assessed by studies of fish bone accumulations.

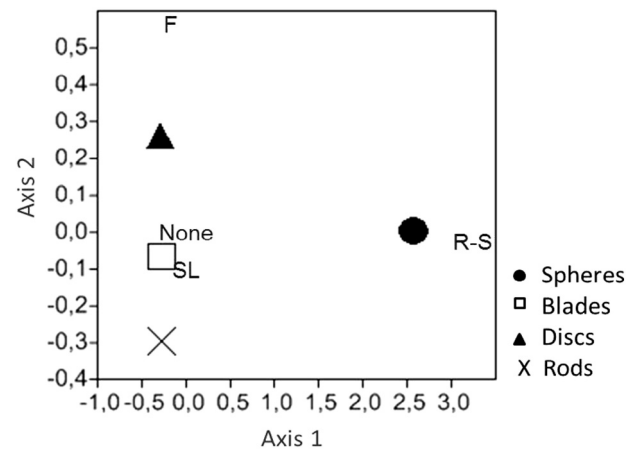


Fig. 7. Correspondence analysis between shape classes and their mode of transport.

As we have seen, bone dispersal process in hydrologic systems can be affected by bone shape, potentially leading to the formation of bone accumulations with differential skeletal part representations. This observation is based on two related factors: 1. fish skeletal parts are represented by different bone morphologies; 2. there are tendencies towards differential hydrologic transportation between fish skeletal elements. Considering the body segments defined by Zohar et al. (2001), Fig. 11 represents the approximate ratios of different shapes that compose each anatomical region in Creole perch. The cranium shows more variability in bone morphology than the appendicular skeleton and vertebral column. Neurocranium and branchial region are composed entirely by blades. This shape is also important in the other cranial sectors. Disc reaches the 50% in hyoid and opercular regions, while this shape is represented by less proportion in the oromandibular region. Rod is only identified in the last anatomical part. In the appendicular skeleton and the vertebral column no variation in shapes is observed; the first anatomical part is integrated by blades and the second by spheres.

In general, our observations of experimental bone transport of Creole perch bones confirm the results from previous experimental studies for mammals: The spherical shapes are most affected by water transport processes, even in streams with low speeds (Dodson, 1973;

⁵ This test was done by using the statistical software R, originally designed by Ross Ihaka and Robert Gentleman.

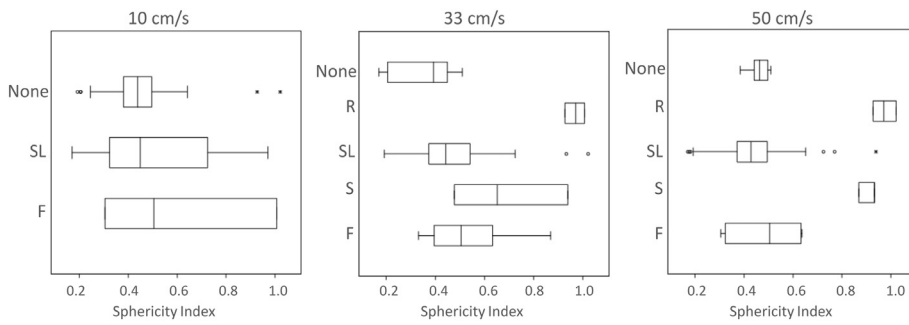


Fig. 8. Sphericity index for each mode of transport at different flow speeds.

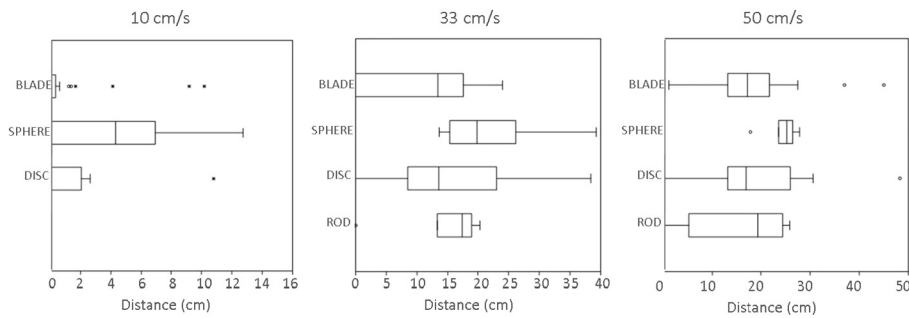


Fig. 9. Distance covered by each shape class at different flow speed.

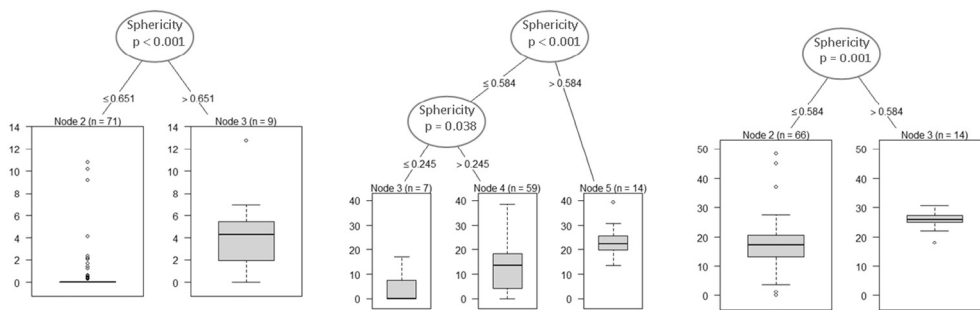


Fig. 10. Regression tree for sphericity and distances for each flow speed.

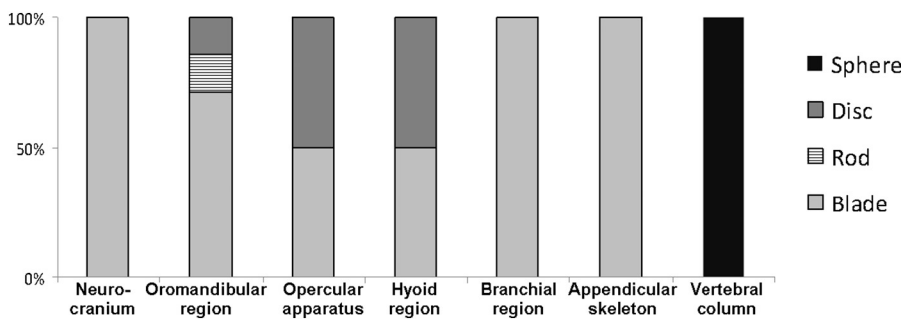


Fig. 11. Representation of shape classes in different fish body parts.

Table 3
Bone density values estimated for *Percichthys trucha* body segments calculated by the water displacement method.

Body segment	g/cm ³
Neurocranium	1.52
Oromandibular region	1.52
Hyoid region	1.35
Branchial region (gill arch)	1.22
Opercular region	1.03
Total cranial	1.28
Appendicular skeleton	1.73
First dorsal spine region	1.26
Vertebral column	1.08
Total postcranial	1.20

Kaufmann and Gutiérrez, 2004). Experiments conducted with mammal bones have shown that light and porous bones, such as vertebrae, are transported farther downstream than heavier bones, such as limb elements (Aslan and Behrensmeier, 1996). Those differences in weight and porosity seem to be also evident between the fish anatomical parts of Creole perch (Table 3). However, some cranial elements (e.g. opercular bones) are transported significant shorter distances than vertebrae with similar bone density, which implies that bone density is not the unique mediator in bone transportation.

This experimental study indicates that hydrologic processes can impose biases giving a unique skeletal element composition in fish bone assemblages. Particularly, the domination or absence of vertebrae in fish bone accumulations is one of the aspects most used in interpretations of archaeological fish assemblages and in discussions on the involved cultural processes (Butler, 1993; Stewart, 1991; Zohar et al.,

Table 4
Groups with high (G1), medium (G2) and low (G3) hydric transport potential considering the shape of the elements commonly identified in the archaeological record.

Shape	G1	G2	G3
Sphere	Caudal vertebra Precaudal vertebra		
Disc	Epiphyal Operculum Hyomandibular	Dentary Parasphenoid	
Blade	Ceratohyal Pharyngeal Articular		Otolith
Blade-disc	Quadrate		
Disc-rod	Basioccipital		
Rod-blade	Vomer		
Rod		Maxilla	

2001). In fact, the absence or complete domination of fish vertebrae is commonly noted in archaeological sites and they normally lead to cultural interpretations in site formation. However, based on the above considerations, the possibility that fluvial processes can lead to deposition and re-deposition of fish vertebrae in time-averaged records should be considered.

As soon as other processes seem to give a similar pattern, leading to a better preservation and/or recovery of vertebrae, equifinality problems should be considered. For example, Nicholson (1992b) has demonstrated experimentally that small and spherical fish bones such as vertebrae may be preserved preferentially during trampling and sedimentary abrasion, while Nagaoka (2005) has shown that spherical elements are one of the most likely shapes to be recovered. The relationship of the bones to the sediments enclosing them and potential signs of transportation such as abrasion should be explored.

4.3. Testing an archaeological case

In order to evaluate the hydrodynamic sorting incidence in ichthyoarchaeological assemblages, a simplified differential transport model is proposed. Elements assigned to the same transport group at least in two different flow velocities were considered and the coincident group was used in model construction. Table 4 lists the anatomical elements assigned to each transport group according to their shapes.

Hydric action moves (erodes) materials from a sector (archaeological sites) and deposits (accumulates) them in another one (re-deposited assemblages). Thus, two main kinds of material records could be expected: a domination of elements assigned to G3 is expected in the first situation, while re-deposited assemblage would be mainly integrated by bones from G1 category.

Medano Ruta 6 (MR-6) is an archaeological open-air site from

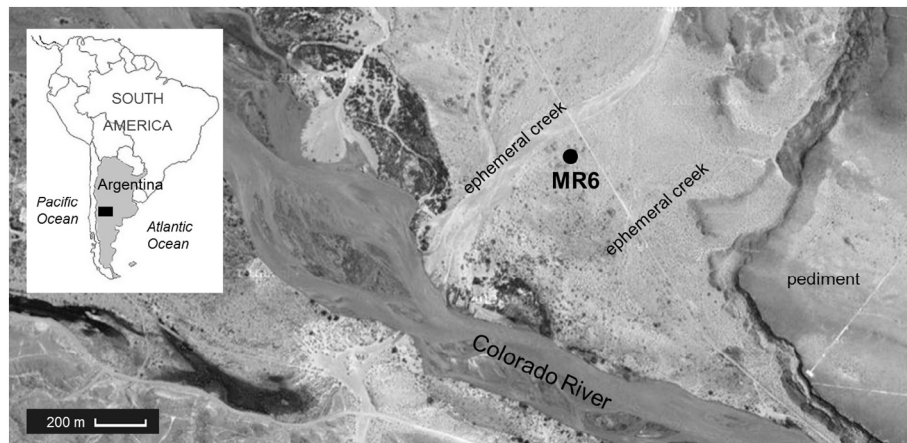


Fig. 12. Location of the Medano Ruta 6 (MR6) site.

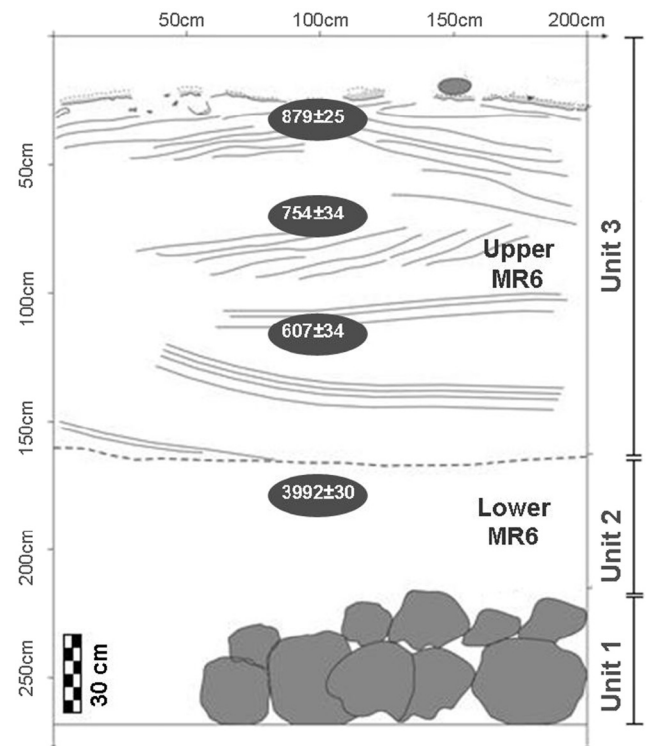


Fig. 13. Stratigraphy and chronological data from the MR6 archaeological site. Modified from Tripaldi et al. (2017). Units 1, 2 and 3 correspond to geomorphologic criteria. Upper and Lower MR6 refer to the archaeological assemblages distinguished at the site.

Central Western Argentina. It is located immediately next to the alluvial plain of the Colorado River, which is ~700 m to the south of this site (Tripaldi et al., 2017) (Fig. 12). The archaeological record at the MR-6 site corresponds to a short term occupation, probably a restricted activity site, and it is mostly composed by faunal remains - such as fish and some mammal bones - Rhea egg shells, lithic artifacts and charcoal (Tripaldi et al., 2017). Geomorphological analysis of this deposit distinguished three sediment units, two of which presented archaeological fish remains: Unit 3 - where upper fish bone assemblage was recovered - was related to an eolian morphogenesis (Tripaldi et al., 2017), so hydric action is not presumed. The lower ichthyoarchaeological assemblage came from Unit 2, which was interpreted as the product of a fluvial current and characterized as a fluvial-eolian interaction facies. In this last case, water is thought to have played an important role in assemblage formation, either as an accumulative agent or as an erosive one. The upper deposit was dated to ca. 800–600 years BP and the lower unit has an estimated chronology of ca. 4000 years BP (C¹⁴; Tripaldi et al.,

Table 5
Taxonomic and anatomic representation (NISP) of the ichthyoarchaeological assemblages from MR6 site, and transport groups assigned to each skeletal element according to the model.

Anatomic unit	Transport group	Upper MR6			Lower MR6	
		<i>Diplomystes</i> sp.	<i>Percichthys</i> sp.	Indet.	<i>Percichthys</i> sp.	Indet.
Articular	G1	0	0	1	0	0
Basioccipital	G1	0	5	0	0	0
Caudal vert.	G1	0	20	5	0	4
Ceratohyal	G1	0	1	1	0	0
Epihyal	G1	0	1	1	0	0
Hyomandibular	G1	0	2	0	0	0
Operculum	G1	0	1	0	0	0
Pharyngeal	G1	0	5	0	0	0
Precaudal vertebra	G1	1	25	0	1	0
Vertebra	G1	1	2	15	0	0
Vomer	G1	0	4	1	0	0
Parasphenoid	G2	0	3	0	0	0
Otolith	G3	0	7	0	3	0
Anguloarticular	-	1	0	0	0	0
Branchial	-	0	5	0	0	0
Cleithrum	-	0	1	0	0	0
Epural/hipural	-	0	3	13	0	0
Ethmoid	-	0	0	1	0	0
Fin rays	-	0	0	12	0	0
Frontal	-	0	6	0	0	0
Hipohyal	-	0	0	1	0	0
Interoperculum	-	1	0	0	0	0
Mesopterigoid	-	0	1	0	0	0
Orbital	-	0	1	0	1	0
Palatine	-	0	3	1	0	0
Posttemporal	-	0	1	0	0	0
Preoperculum	-	0	1	0	0	0
Rib	-	0	0	3	0	0
Spine	-	0	1	4	0	0
Supraoccipital	-	0	2	1	0	0
Urohyal	-	0	1	0	0	0
Weber apparatus	-	1	0	0	0	0
Indet.	-	0	0	101	0	0
Total	-	5	102	161	5	4

2017) (Fig. 13). Further information about the recovery and analysis of the assemblages from MR6 is discussed elsewhere (Corbat, 2016). Same techniques, including a 2 mm screen size, were used to recover the faunistic material from both units. Fragmentation index (WMI; sensu Zohar et al., 2001) estimated for Upper and Lower MR6 are not significantly different ($t = 0.45$; $p > 0.05$) and are relatively high (78.6% y 75.0%, respectively).

Unit 1 has been related to the action of high energy streams and it has no archaeological evidence (Tripaldi et al., 2017). *Percichthys trucha* is the dominant taxa among the identified specimens from the upper context of MR6 (Table 5). Thus, all anatomically identified elements - considered in the model - were used in this analysis. The majority of the assemblage was taxonomically unidentified, but most of it could be identify to elements, and then incorporated to the analysis.

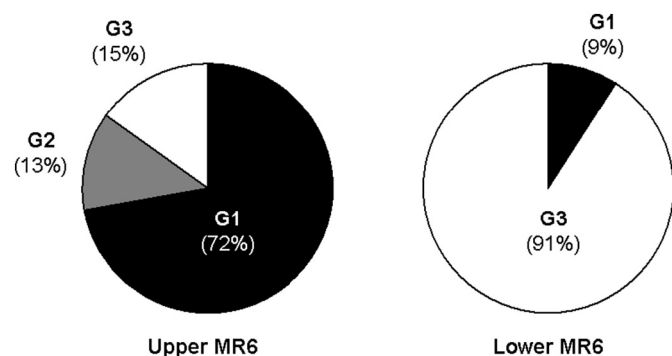


Fig. 14. Elements representation regarding transport groups in the upper and lower ichthyoarchaeological assemblages from MR6.

Fig. 14 illustrates the relative abundance of elements by transport group representations in both archaeological assemblages from MR6. Anatomic data related to each transport group is detailed in Supplemental file 2. The lower unit is dominated by G3 elements; almost all of the more easily transported elements (G1) have been removed, remaining mainly those transported with the greatest difficulty. Given the geomorphological information of the MR6 lower assemblage, a bone removing process by hydric transportation should be significantly considered in the formation process of this deposit.

Clearly this interpretation cannot be stated in an isolated way from other potential time-averaging processes (Nicholson, 1992a), and two factors related to bone survival should also be taken into account. On the one hand, > 3000 years separate the archaeological deposits at MR6. On the other hand, most of the elements recovered from Unit 2 are those with the highest mineral density (otoliths) (Falabella et al., 1994). Under these circumstances, a differential preservation in favor of the most recent context should be expected. However, the fact that bone elements with low density values, such as vertebrae, were also recovered in Unit 2 (Fig. 14) indicates that this process did not imperatively determine the composition of the ichthyoarchaeological assemblage, so the anatomical profile recorded in this ichthyoarchaeological record should be mainly explained by hydric action.

5. Summary and conclusion

Shape has an important role in zooarchaeological assemblages' formation, together with density and size. However, it has been poorly studied, specifically in fishes. This article presents quantitative and qualitative data on fish bone morphology and explores its incidence in hydric transport processes, and eventually in the composition of

ichthyoarchaeological assemblages. Intra-specific variability was sampled by analyzing 25 anatomic elements from 30 Creole perches.

Trends can be observed in relation to the type of movement undertaken by different shapes, especially as flow velocity increases, when spheres tend to move by rolling or saltation, and other shapes do it sliding or floating. On the other hand, shape of the element has a stronger incidence on the transported distance. Spheres have the greatest transport potential, followed by discs, blades, and finally rods. Elements with higher sphericity values tend to move faster particularly as flow velocity increases. This study has shown that potential post-depositional processes can produce biases on archaeological assemblages, giving them unique skeletal composition and similar to those expected from cultural processes.

This is a first approximation to the study of hydrodynamic transport of fish bones considering the shape of anatomical elements. Therefore, research on other species is needed to ensure that the context in which this research is applicable is fully realized. On the same way, much work needs to be done in order to explore how other elements (e.g. complete vertebrae, other precaudal vertebrae, articulated bones) are affected by the same process and what happens under different conditions (e.g. different sedimentary surfaces; other initial positions of the bones, elements under water saturation).

Results derived from this experiment are not strictly valid over much of the range of natural conditions (Aslan and Behrensmeier, 1996). Nevertheless, following Hanson (1980), they yield better approximations of fish bone behaviour than previously available and provide a rational baseline which can be empirically tested and refined.

Supplementary data to this article can be found online at <http://dx.doi.org/10.1016/j.jasrep.2017.05.056>.

Funding

The research was developed under the project PICT 2012-1015 and was partially funded by CONICET grants.

Acknowledgements

To Adolfo Gil, Gustavo Neme, Laura Salgán, Sergio Bogan and Agustina Zangrando. We would like to thank to the Dirección Provincial de Recursos Naturales, Delegación Malargüe, and to Pardo and Pérez families. We specially thank Ing. Roberto Biondi, Nicolás Membrive and the hydraulic area of the Universidad Tecnológica Nacional for helping us use the flume channel, as well as María de la Paz Pompei, María Gutiérrez, Cristian Kaufmann and Marcelo Cardillo, whose collaboration we deeply appreciate. Two anonymous reviewers improved the original manuscript. Nevertheless, the content of this article remains entirely our responsibility.

References

Aslan, A., Behrensmeier, A.K., 1996. Taphonomy and time resolution of bone assemblages in a contemporary fluvial system: the East Fork River, Wyoming. *PALAIOS* 11, 411–421. <http://dx.doi.org/10.2307/3515209>.

Behrensmeier, A.K., 1975. The taphonomy and paleoecology of plio-pleistocene vertebrate assemblages east of lake Rudolf, Kenya. *Bull. Mus. Comp. Zool.* 146, 473–578.

Blatt, H., Middleton, G., Murray, R., 1980. *Origin of Sedimentary Rocks*. Prentice-Hall, Inc., New Jersey.

Boaz, N.T., Behrensmeier, A.K., 1976. Hominid taphonomy: transport of human skeletal parts in an artificial environment. *Am. J. Anthropol.* 45, 53–60.

Butler, V., 1993. Natural versus cultural salmonid remains: origin of the Dalles readout bones, Columbia River, Oregon, USA. *J. Archaeol. Sci.* 20, 1–24. <http://dx.doi.org/10.1006/jasc.1993.1001>.

Butler, V., 1996. Tui chub taphonomy and the importance of marsh resources in the western great basin of North America. *Am. Antiq.* 61, 699–717. <http://dx.doi.org/10.2307/282012>.

Butler, V., Chatters, J., 1994. The role of bone density in structuring prehistoric salmon bone assemblages. *J. Archaeol. Sci.* 21, 413–424. <http://dx.doi.org/10.1006/jasc.1994.1039>.

Coard, R., 1999. One bone, two bones, wet bones, dry bones: transport potentials under experimental conditions. *J. Archaeol. Sci.* 26, 1369–1375. <http://dx.doi.org/10.1006/jasc.1999.0438>.

Coard, R., Dennell, R.W., 1995. Taphonomy of some articulated skeletal remains: transport potential in an artificial environment. *J. Archaeol. Sci.* 22, 441–448. <http://dx.doi.org/10.1006/jasc.1995.0043>.

Colley, S., 1990. The analysis and interpretation of archaeological fish remains. In: Schiffer, M.B. (Ed.), *Archaeological Method and Theory 2*. Academic Press, San Diego, pp. 207–253.

Corbat, M., 2016. Variabilidad ambiental y sociocultural en la explotación de peces en el centro-occidente argentino: una evaluación zooarqueológica. (Thesis presented for the degree of Doctor in Archaeology) Universidad de Buenos Aires, Argentina.

Corbat, M., Zangrando, A.F., 2012. Una aproximación tafonómica a los restos de peces en Laguna Llancanelo. II Encuentro Latinoamericano de Zooarqueología, Santiago de Chile, Chile.

Darwent, Ch., Lyman, R., 2002. Detecting the postburial fragmentation of carpals, tarsals, and phalanges. In: Haglund, W.D., Sorg, M.H. (Eds.), *Advances in Forensic Taphonomy: Method, Theory, and Archaeological Perspectives*. CRC Press, Boca Raton, Florida, pp. 355–377.

Dodson, P., 1973. The significance of small bones in paleoecological interpretation. *Contrib. Geol.* 12, 15–19.

Falabella, F., Vargas, M.L., Meléndez, R., 1994. Differential preservation and recovery of fish remains in Central Chile. In: Van Neer, W. (Ed.), *Fish Exploitation in the Past. Proceedings of the 7th Meeting of the ICAZ Fish Remains Working Group*, Annales du Musée Royal de l'Afrique Centrale, Sciences Zoologiques 274, Tervuren, pp. 25–35.

Frostick, L., Reid, I., 1983. Taphonomic significance of sub-aerial transport of vertebrate fossils on steep semi-arid slopes. *Lethaia* 6, 157–164.

Gifford-Gonzalez, D., Stewart, K., Rybczynski, N., 1999. Human activities and site formation at modern lake margin foraging camps in Kenya. *J. Anthropol. Archaeol.* 18, 397–440. <http://dx.doi.org/10.1006/jaa.1999.0337>.

Grayson, D.K., 1988. Danger cave, last supper cave, and hanging rock shelter: the faunas. *Anthropol. Pap. Am. Mus. Nat. Hist.* 66 (1), 1–130.

Hammer, Ø., Harper, D., Ryan, P., 2001. PAST: paleontological statistics software package for education and data analysis. *Palaeontol. Electron.* 4, 1–9.

Hanson, B., 1980. Fluvial taphonomic processes: models and experiments. In: Behrensmeier, A., Hill, A. (Eds.), *Fossils in the Making. Vertebrate Taphonomy and Paleoecology*. The University of Chicago Press, Chicago, pp. 156–181.

Kaufmann, C., Gutiérrez, M., 2004. Dispersión potencial de huesos de guanaco en medios fluviales y lacustres. Aproximaciones Contemporáneas a la Arqueología Pampeana. In: Martínez, G., Gutiérrez, M.A., Curtoni, R., Berón, M., Madrid, P. (Eds.), *Perspectivas teóricas, metodológicas, analíticas y casos de estudio*. Facultad de Ciencias Sociales, UNCPBA, Olavarría, pp. 129–146.

Kaufmann, C., Gutiérrez, M.A., Álvarez, M.C., González, M., Massigoge, A., 2011. Fluvial dispersal potential of guanaco bones (*Lama guanicoe*) under controlled experimental conditions: the influence of age classes to the hydrodynamic behaviour. *J. Archaeol. Sci.* 38, 334–344. <http://dx.doi.org/10.1016/j.jas.2010.09.010>.

Lubinski, P., 1996. Fish heads, fish heads: an experiment on differential bone preservation in a salmonid fish. *J. Archaeol. Sci.* 23, 175–181. <http://dx.doi.org/10.1006/jasc.1996.0015>.

Lyman, R., 1984. Bone density and differential survivorship of fossil classes. *J. Anthropol. Archaeol.* 3, 259–299. [http://dx.doi.org/10.1016/0278-4165\(84\)90004-7](http://dx.doi.org/10.1016/0278-4165(84)90004-7).

Lyman, R., 1985. Bone frequencies: differential transport, in-situ destruction, and the MGUI. *J. Archaeol. Sci.* 12, 221–236. [http://dx.doi.org/10.1016/0305-4403\(85\)90022-6](http://dx.doi.org/10.1016/0305-4403(85)90022-6).

Nagaoka, L., 2005. Differential recovery of Pacific Island fish remains. *J. Archaeol. Sci.* 32, 941–955. <http://dx.doi.org/10.1016/j.jas.2004.12.011>.

Nicholson, R., 1992a. An assessment of the value of bone density measurements to archaeoichthyological studies. *Int. J. Osteoarchaeol.* 2, 139–154. <http://dx.doi.org/10.1002/oa.1390020206>.

Nicholson, R., 1992b. Bone survival: the effects of sedimentary abrasion and trampling on fresh and cooked bone. *Int. J. Osteoarchaeol.* 2, 79–90. <http://dx.doi.org/10.1002/oa.1390020110>.

Nicholson, R., 1993. A morphological investigation of burnt animal bone and an evaluation of its utility in archaeology. *J. Archaeol. Sci.* 20, 411–428. <http://dx.doi.org/10.1006/jasc.1996.0049>.

Nicholson, R., 1996. Bone degradation, burial medium and species representation: debunking the myths, an experiment-based approach. *J. Archaeol. Sci.* 23, 513–533. <http://dx.doi.org/10.1006/jasc.1996.0049>.

Nicholson, R., 1998. Bone degradation in a compost heap. *J. Archaeol. Sci.* 25, 393–403. <http://dx.doi.org/10.1006/jasc.1997.0208>.

Pante, C.P., Blumenschine, R.J., 2010. Fluvial transport of bovid long bones fragmented by the feeding activities of hominins and carnivores. *J. Archaeol. Sci.* 37, 846–854. <http://dx.doi.org/10.1016/j.jas.2009.11.014>.

Stahl, P., 1996. The recovery and interpretation of microvertebrate bone assemblages from archaeological contexts. *J. Archaeol. Method Theory* 3, 31–75.

Stewart, K.M., 1991. Modern fishbone assemblages at Lake Turkana, Kenya: a methodology to aid in recognition of hominid fish utilization. *J. Archaeol. Sci.* 18, 579–603. [http://dx.doi.org/10.1016/0305-4403\(91\)90054-S](http://dx.doi.org/10.1016/0305-4403(91)90054-S).

Stewart, K., Gifford-Gonzalez, D., 1994. An Ethnoarchaeological contribution to identifying hominid fish processing sites. *J. Archaeol. Sci.* 21, 237–248. <http://dx.doi.org/10.1006/jasc.1994.1024>.

Stewart, K., Gifford-Gonzalez, D., Rybczynski, N., 1997. Characteristics of modern foraging camps and their faunas from Lake Turkana, Kenya. *Anthropozoologica* 25–26, 763–766.

Trapani, J., 1998. Hydrodynamic sorting of avian skeletal remains. *J. Archaeol. Sci.* 25, 477–487. <http://dx.doi.org/10.1006/jasc.1997.0257>.

Tripaldi, A., Zárate, M., Neme, G., Gil, A., Salgán, L., 2017. Archaeological site formation processes in northwestern Patagonia, Mendoza Province, Argentina. *Geoarchaeology*

- (In press). <http://dx.doi.org/10.1002/gea.21632>.
- Voorhies, M.R., 1969. Taphonomy and population dynamics of an early Pliocene vertebrate fauna, Knox County, Nebraska. University of Wyoming. Contrib. Geol. 1, 1–69 (Special Paper).
- Wainwright, P., 2005. Functional morphology of the pharyngeal jaw apparatus. Fish Biomech. 23, 77–101.
- Wheeler, A., Jones, A.K., 1989. Fishes. Cambridge University Press, Cambridge.
- Zingg, T., 1935. Beitrage zur Schotteranalyse. Schweiz. Mineral. Petrogr. Mitt. 15, 39–140.
- Zohar, I., Belmaker, M., 2005. Size does matter: methodological comments on sieve size and species richness in fishbone assemblages. J. Archaeol. Sci. 32, 635–641. [http://dx.doi.org/10.1016/S0305-4403\(03\)00037-2](http://dx.doi.org/10.1016/S0305-4403(03)00037-2).
- Zohar, I., Biton, R., 2011. Land, lake, and fish: investigation of fish remains from Gesher Benot Ya'akov (paleo-Lake Hula). J. Hum. Evol. 60, 343–356.
- Zohar, I., Cooke, R., 1997. The impact of salting and drying on fish bones: preliminary observations on four marine species from Parita Bay, Panama. Archaeofauna 6, 59–66.
- Zohar, I., Dayan, T., Galili, E., Spanier, E., 2001. Fish processing during the early Holocene: a taphonomic case study from coastal Israel. J. Archaeol. Sci. 28, 1041–1053. <http://dx.doi.org/10.1006/jasc.2000.0630>.
- Zohar, I., Belmaker, M., Nadel, D., Gafny, S., Goren, M., Hershkovitz, I., Dayan, T., 2008. The living and the dead: how do taphonomic processes modify relative abundance and skeletal completeness of freshwater fish? Palaeogeogr. Palaeoclimatol. Palaeoecol. 258, 292–316.